

# Failure Precursor Identification and Degradation Modeling for Insulated Gate Bipolar Transistors Subjected to Electrical Stress

Junmin Lee<sup>1</sup>, Hyunseok Oh<sup>2</sup>, Chan Hee Park<sup>3</sup>, Byeng D. Youn<sup>4</sup>, Deog Hyeon Kim<sup>5</sup>, Byung Hwa Kim<sup>6</sup>, and Yong Un Cho<sup>7</sup>

<sup>1,2,3,4</sup>*Department of Mechanical Engineering, Seoul National University, Seoul, 08826, Republic of Korea*

*l3jmlee@gmail.com  
hsoh52@hotmail.com  
pchee93@snu.ac.kr  
bdyoun@snu.ac.kr*

<sup>5,6,7</sup>*Equipment Control Engineering Team 1, Production and Development Division, Hyundai Motor Group, Ulsan, Republic of Korea*

*dhkims@hyundai.com  
axa@hyundai.com  
cyongun@hyundai.com*

## ABSTRACT

In driving equipment of smart factories, unexpected failures of insulated gate bipolar transistors (IGBTs) are often observed. Electrical stresses are one of the dominant causes for the IGBT failures in the field. However, there is little study about the effect of electrical stresses on the degradation of IGBTs. In this paper, we attempt to identify a key failure precursor for IGBTs subjected to electrical stresses and to model the evolution of the failure precursor. To achieve the goals, first, the main causes of IGBT failures are identified based on maintenance history, filed failure data, and experts' opinions. Second, an artificial fault injection method, i.e., electrostatic discharge (ESD), is employed to produce partially degraded (but not failed) IGBTs. The proper levels of the intensity of electrical loads (i.e., magnitude and number of the ESDs) are also determined. Finally, artificial ESD faults are seeded to IGBTs and potential candidates of failure precursors are measured. The steps are repeated until the failure of the IGBTs is observed. A relevant failure precursor is determined based on the results. A degradation model for the precursor is then built. It is expected that the key failure precursor determined in this study and the proposed degradation model can help avoid unexpected failure of IGBTs in driving equipment of smart factories.

## 1. INTRODUCTION

IGBTs are a transistor that combines the characteristics of metal oxide semiconductor field effect transistors

(MOSFETs) and bipolar junction transistors (Baliga, Adler, Love, Gray, & Zommer, 1984). With the increased use of IGBTs in various fields, the reliability of IGBTs became critical. According to the industry-based survey of reliability in power electronic converters (Yang, Bryant, Mawby, Xiang, Ran, & Tavner, 2011), more than 30% of responders selected power devices as the most fragile components and IGBTs were most used power devices (more than 40 %). An unexpected failure of IGBTs in safe- or mission-critical system could lead to catastrophic failures and immense amount of losses.

Numerous studies were conducted on physics of failure, condition monitoring, and prognostic of IGBTs. Dominant failure mechanisms include fatigue, latch-up, electrostatic discharge (ESD), radiation-induced effect, and ceramic substrate fracture (Oh, Han, McCluskey, Han, & Youn, 2015). Fatigue failure can occur due to the thermal cycling (Celnikier, Benabou, Dupont, & Coquery, 2011), while latch-up can happen due to mishandling of the devices (Jeong, Hong, & Park, 2007). From maintenance histories in the field, electrical overloads that exceed the maximum rating of IGBTs for very short duration were reported to be most predominant (Lee, Oh, Park, Youn, Kim, Kim, & Cho, 2016). They were attributed to various factors such as intermittent blackout, falling of thunderbolt, or reverse current during emergency stop. The damage accumulated by electrical overloads can lead to the unexpected failure of the IGBTs. Latent and intermittent damages by electrical stresses on power devices were studied by Wysocki, Vashchenko, Celaya, Saha, and Goebel (2009). They injected ESDs to the junctions of power devices, and compared electrical characteristics of the IGBTs before and after the injection of

Junmin Lee et al. This is an open-access article distributed under the terms of the Creative Commons Attribution 3.0 United States License, which permits unrestricted use, distribution, and reproduction in any medium, provided the original author and source are credited.

ESDs. However, their study did not investigate the effect of ESDs on the degradation of IGBTs.

Various failure precursors were examined in conjunction with failure sites and failure mechanisms as shown in Table 1 and 2 (Oh et al., 2015). Patil, Celaya, Das, Goebel, and Pecht (2009) examined the conditions of IGBTs in the aging tests and then, determined failure precursors. Gate-emitter threshold voltage ( $V_{th}$ ) was observed to be a precursor for gate oxide degradation, and collector-emitter ON voltage ( $V_{CE(on)}$ ) and turn-off time ( $t_{off}$ ) was observed to be a precursor for die-attach degradation. Zhou, Zhou, and Sun (2013) detected defects in IGBT modules by identifying the dynamic change of the gate current ( $I_G$ ). Zhou, Zhou, and Xu (2013) observed the change of gate voltage oscillation before and after partial bond wires lift off of IGBT modules. However, most of the previous studies observed the change of the precursor or characteristics just between before and after aging. To the best of our knowledge, there is no study on the degradation of IGBTs subjected to electrical stresses and the modeling of the degradation.

Table 1. The definitions of failure precursors for IGBTs

Symbol	Definition
$V_{GE}$	Gate-emitter voltage
$V_{GE(th)}$	Gate-emitter threshold voltage
$V_{CE(on)}$	Collector-emitter On voltage
$t_{on}$	turn-on time
$t_{off}$	turn-off time
$R_{th}$	Thermal resistance from junction to case
$T_j$	Junction temperature

Table 2. Failure sites, mechanisms, and precursors of IGBTs

Failure sites	Failure Mechanisms	Failure precursors
Die	Latch-up and secondary breakdown	$V_{GE(th)}$ $V_{CE(on)}$ $t_{off}$
	Time dependent dielectric breakdown	$V_{GE(th)}$ $V_{GE}$
Bonding wire	Fatigue and/or reconstruction	$t_{on}$ $t_{off}$ $V_{CE(on)}$ $V_{GE}$
Solder joint	Fatigue or grain growth	$R_{th}$ $V_{CE(on)}$ $t_{off}$ Low-order harmonics

The objective of this paper is to determine the key failure precursor and corresponding model that predicts the degradation of IGBTs subjected to electrical stresses. To achieve the objective, the remaining sections of this paper are organized as follows. Section 2 describes the experimental setup and procedures for accelerated testing by ESDs. Section 3 determines a potential failure precursor based on the test results. Section 4 presents a degradation model related to the

key failure precursor. This paper concludes with future works in Section 5.

## 2. EXPERIMENTAL SETUP AND PROCEDURES

### 2.1. Test Sample and Equipment

The test samples are trench gate field stop IGBTs; three sets of IGBT components (Infineon Technologies-IKP10N60T, Infineon Technologies-IGW60T120, Fuji Electric-IGW60T120) and one set of IGBT module (Semikron-SEMiX101GD126HDs). The IGBTs are indicated as C1, C2, C3, and M1 below. The specifications of the IGBT components and module are shown in Table 3.

Table 3. Maximum ratings of IGBTs

Parameter	C1	C2	C3	M1
$V_{CES}$ (V)	600	1200	600	1200
$I_C$ (A)	10	60	35	75
$T_j$ (°C)	175	150	175	150

$V_{CES}$ : collector-emitter voltage

Two different equipment was used to characterize the IGBTs. A curve tracer, Tektronix 370B, was used to monitor the current-voltage characteristics of IGBT components. A customized equipment was used to monitor the electrical characteristics of IGBT modules. Figure 1 illustrates a schematic diagram of the equipment that is composed of a desktop computer, oscilloscope (Keysight, DSOX4034A), function generator (Keysight, 33210A), and an AVR<sup>®</sup> control board. The collector-emitter switch-off voltage ( $V_{CE(off)}$ ) and the maximum collector current ( $I_C$ ) of the AVR<sup>®</sup> board are 24 V and 20 A, respectively.



Figure 1. Experimental setup for module testing

The operation of the module testbed is illustrated below. First the AVR<sup>®</sup> board makes an electrical potential between the collector and the emitter, i.e.,  $V_{CE(off)}$ . Then, the function generator produces gate input signals that is transferred to the AVR<sup>®</sup> board, and it is converted to square signals required for the gate control of IGBTs, i.e., ON/OFF control. While the IGBT is switched between on and off, the oscilloscope measures voltage and current waveforms of the IGBT;

collector voltage ( $V_C$ ), gate voltage ( $V_G$ ), emitter voltage ( $V_E$ ), and collector current ( $I_C$ ). At the same time, the desktop computer gathers, saves, and displays all the information.

An ESD simulator (Noiseken, ESS-2000 & TC-815R) was used to induce a degradation and a failure to the IGBTs. The ESD simulator has three parameters; discharge voltage, number of discharges, and interval. The discharge voltage is the peak voltage of ESD pulses and the interval is the duration of discharge. For example, the discharge voltage, number of discharges, and interval can be set to be 1200 V, 300, and one second, respectively. This implies that 1200 V ESDs with the duration of one second are discharged 300 times. The test setup for ESD injection was referred to the standard test (IEC-61000-4-2).

The most probable junctions that tend to be exposed to electrical overload were discussed with field experts. As the gate lead of IGBTs is rarely exposed to the overload, the combination of the gate-emitter (G-E) and gate-collector (G-C) junctions were excluded. In addition, as the gate oxide degradation is known to be irrelevant to collector-emitter stress, the C-E and E-C junctions were also excluded. Hence, C-G and E-G junctions were determined as potential candidates to emulate an ESD-related failure in the field. In this study, the ESDs were injected to the C-G junction.

## 2.2. Experimental Procedures

The procedures of the test was illustrated in Figure 2. After a certain number of ESDs are discharged (stepsize) with a certain interval, the characteristics of IGBTs are measured using the curve tracer (component) or the testbed (module). Both the “ESD injection” and “Measure” phases in Figure 2 was repeated until IGBTs failed.

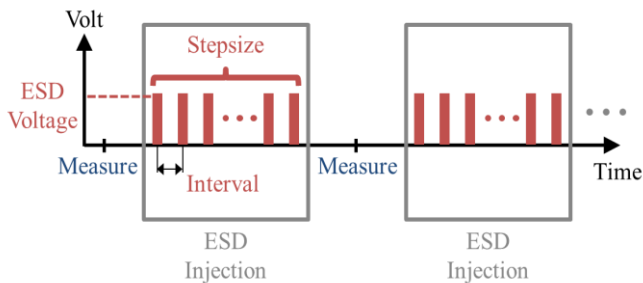


Figure 2. Test procedures

An experimental design in this study was based on two hypotheses; one that the effect of ESD to IGBT is independent on the ESD parameters, and the other that degradation behaviors are consistent among IGBTs whose applied technologies are same; trench gate filed stop. Four test sets were listed in Table 4: a test set using C1, C2, C3, and M1, respectively. The characteristics of IGBTs were measured by the curve tracer in the test set I, II, and III, while

they were measured by the module testbed in the test set IV. The same ESD simulator was used in all the test sets. The first hypothesis was confirmed from test set I; the effects of ESD parameters. The second hypothesis was confirmed with the other sets of tests; the consistency of degradation behaviors among IGBTs with same technology that are subjected to the ESDs. The details are followed in the next section.

## 3. TEST RESULTS

A gate-emitter threshold voltage ( $V_{GE(th)}$ ) was considered a potential precursor.  $V_{GE(th)}$  can be defined based on the constant current method:  $V_G$  when  $I_C$  exceeds a certain threshold value ( $I_{C(th)}$ ). In this study,  $V_{GE(th)}$  of all the samples was normalized using their initial values.

In the component test, multiple I-V curves for several gate voltage were obtained using the curve tracer.  $I_C$  become saturated when  $V_{CE}$  increases. We could determine  $V_{GE(th)}$  by reading a gate voltage when  $I_C$  equals to  $I_{C(th)}$  in the saturation region. In the module-level test, on the other hand,  $V_{GE(th)}$  was extracted based on the constant current method using the measured values ( $V_C$ ,  $V_E$ ,  $V_G$ , and  $I_C$ ) from the module testbed. In Figure 3, the blue line is  $V_C$ ; the green line is  $V_E$ ; the yellow line is  $V_G$ ; and the pink line is  $I_C$ . This plot was obtained when an IGBT was turned on.

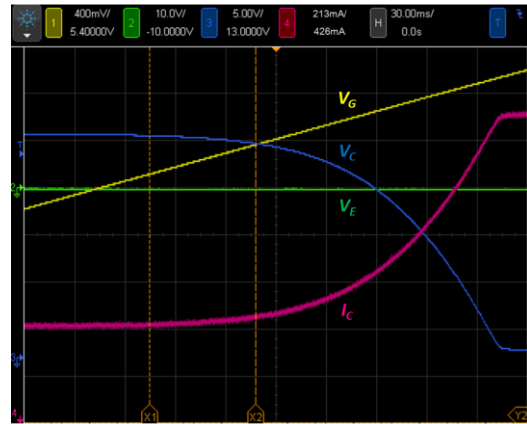


Figure 3. Measured values ( $V_C$ ,  $V_E$ ,  $V_G$ , and  $I_C$ ) from the oscilloscope (DSOX4034A)

All the conducted tests were listed in Table 4. It illustrates test set number, test product name, test index, settings of ESD parameters, and the total number of ESDs for each tests. The effects of the stepsize and interval were verified using tests from C1-1 to C1-4 and from C1-2 to C1-7, respectively. In Figure 4(a), all the degradation behaviors of  $V_{GE(th)}$  were consistent regardless to the different stepsize and/or interval. The effect of the ESD voltage was verified using tests from C1-2 to C1-4 and from C1-8 to C1-13. As the ESD voltage increased, the degradation rate also increased (Figure 4(b)).

Table 4. Conducted test sets

Test set number	Test product	Test index	Parameters of ESD simulator			Total number of ESDs
			ESD Voltage (V)	stepsize	interval (sec.)	
I	C1	C1-1	1000	300	1	6100
		C1-2		18000		
		C1-3		16200		
		C1-4		18000		
		C1-5		19800		
		C1-6		18900		
		C1-7		18900		
		C1-8	900	900	1	22500
		C1-9				22500
		C1-10				21600
		C1-11	1100	900	1	6300
		C1-12				1800
		C1-13				3600
II	C2	C2-1	1800	900	1	18900
		C2-2	2000			14400
		C2-3	2200			12600
III	C3	C3-1	1200	21600	1	129600
		C3-2				136800
		C3-3				93600
IV	M1	M1-1	2400	900	1	9000
		M1-2				8100
		M1-3				8100

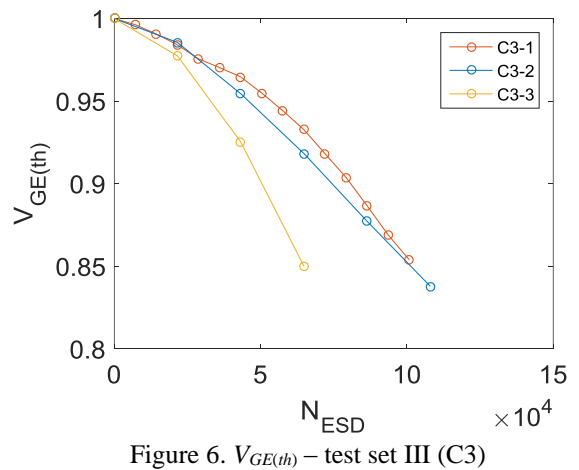
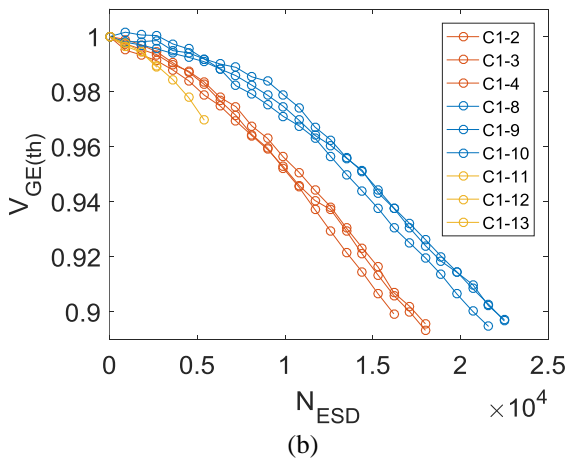
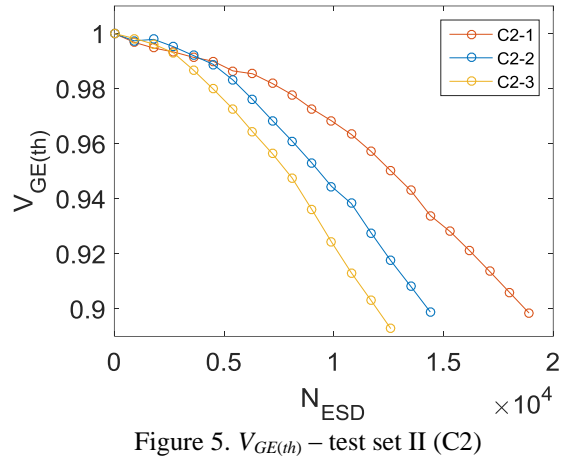
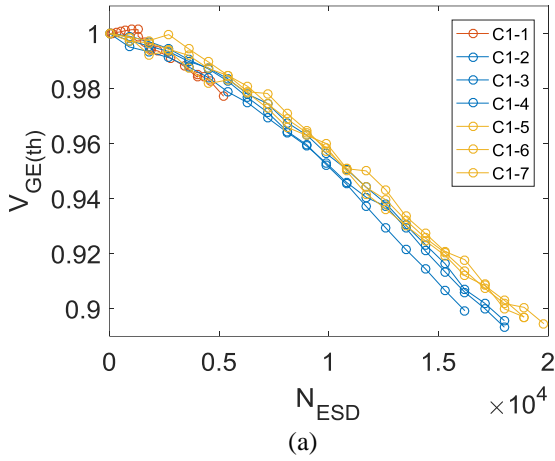
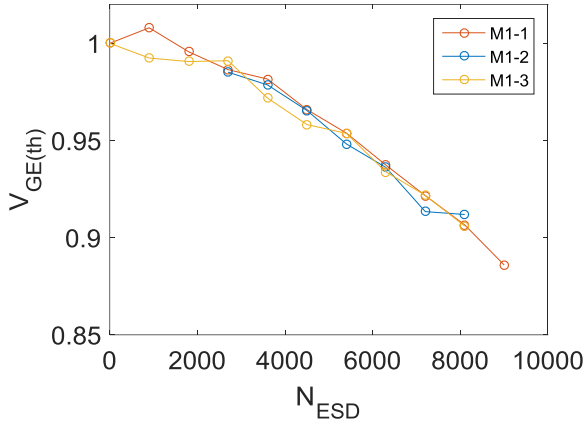


Figure 4.  $V_{GE(th)}$  – test set I (C1): (a) ESD stepsize and interval, (b) ESD voltage

Figure 7.  $V_{GE(th)}$  – test set IV (M1)

The same phenomena was observed from the results of the test set II (Figure 5). On the other hand, C3 showed inconsistent degradation patterns despite the same ESD voltage (Figure 6), while M1 showed consistency like C1 and C2 (Figure 7).

The performance of  $V_{GE(th)}$  was verified for various IGBTs (C1, C2, C3, and M1). With  $V_{GE(th)}$ , the degradation patterns of IGBTs were consistent despite the various electrical load profiles was applied by controlling ESD stepsize and interval. In addition, the increased degradation rates of IGBTs were detected by  $V_{GE(th)}$  when the intensity of electrical load, i.e., ESD voltage, increased.

Failure analysis was conducted for one sample of C1 that failed due to the ESD. The analysis was operated by three steps; a decapsulation, an emission, and a delayer. In the decapsulation step, the plastic compounds and silicone gels that cover and protect an IGBT chip were eliminated. In the emission step, the hot spot was identified by detecting the infrared rays emitted by heat generated from a failure point. In the delayer step, a passivation and metal layers were eliminated. Finally, a contact spike was detected in IGBT chip (Figure 8). In other words, a presence of degradation was verified when IGBT failed due to the ESD.

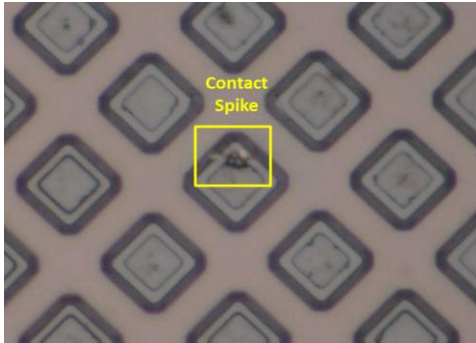


Figure 8 Failure analysis of IGBT

#### 4. DEGRADATION MODELING

The extracted precursor,  $V_{GE(th)}$ , was validated through the experimental data. A degradation model for the precursor was constructed. In the literature, Shringarpure, Venugopal, Li, Clark, Allee, Bawolek, and Toy (2007) developed an experimental equation for the degradation of threshold voltage ( $\Delta V_{th}$ ) in hydrogenated amorphous silicon thin-film transistors (TFTs) like Eq. (1) below.

$$\Delta V_{th}(t) = A \cdot \exp(-E_A/kT) \cdot t^\beta \cdot (V_{GS} - \eta V_{DS} - V_{th,0})^n \quad (1)$$

where  $A$  is the degradation rate;  $E_A$  is the mean of activation energy;  $k$  is the Boltzmann constant;  $T$  is the absolute temperature;  $t$  is the bias stress time duration;  $\beta$  and  $n$  are the process-related coefficients;  $V_{GS}$  is the gate-source voltage;  $V_{DS}$  is the drain-source voltage; and  $V_{th,0}$  is the initial threshold voltage. The  $\eta V_{DS}$  is related to decline of carriers when the transistor reaches to the saturation point. In this equation, the  $\exp(-E_A/kT)$  represents the effect of temperature and the  $(V_{GS} - \eta V_{DS} - V_{th,0})$  can be regarded as a kind of electrical stress level applied to the transistor.

This degradation model was used to predict the behavior of the IGBT with some modifications; the  $\exp(-E_A/kT)$  was assumed to be a constant value as the measured ambient temperature did not change.  $V_{DS}$  was substituted with  $V_{GE}$ , and the stress level  $(V_{DS} - \eta V_{DS} - V_{th,0})$  was a function of the ESD voltage. The stress time ( $t$ ) was substituted with the number of ESD injection. The modified degradation model for IGBTs was given below.

$$\Delta V_{GE(th)}(N_{ESD}) = A \cdot (N_{ESD})^\beta \cdot (V_{ESD} - V_{rated})^n \quad (2)$$

where  $\Delta V_{GE(th)}$  represents the change of the gate-emitter threshold voltage;  $N_{ESD}$  is the applied number of ESD;  $A$  is the degradation rate;  $\beta$  and  $n$  are the process-related coefficients;  $V_{ESD}$  is the ESD voltage; and  $V_{rated}$  is the maximum rated voltage of IGBTs. Then a model for  $V_{GE(th)}$  was constructed using  $\Delta V_{GE(th)}$  from Eq. (2).

$$\begin{aligned} V_{GE(th)}(N_{ESD}) &= \frac{V_{GE(th),0} - \Delta V_{GE(th)}(N_{ESD})}{V_{GE(th),0}} \\ &= 1 - \frac{A \cdot (N_{ESD})^\beta \cdot (V_{ESD} - V_{rated})^n}{V_{GE(th),0}} \\ &= 1 - A' \cdot (N_{ESD})^\beta \cdot (V_{ESD} - V_{rated})^n \end{aligned} \quad (3)$$

where  $V_{GE(th)}$  is the normalized gate-emitter threshold voltage;  $V_{GE(th),0}$  is the initial gate-emitter threshold voltage;  $A$  is the degradation rate;  $\beta$  and  $n$  are the process-related coefficients; and  $A'$  is the adjusted degradation rate. In this study, the process-related coefficients ( $\beta$  and  $n$ ) were regarded as constants among all the IGBTs as they were manufactured with the same technologies. In addition, the adjusted degradation rate ( $A'$ ) is regarded as the material-dependent factor that reflects the variations of the degradation rate

among the manufacturing companies. After we fitted  $A'$ ,  $\beta$ ,  $n$  based on the data sets of C1 and C2, the  $A'$  for C3 and M1 were fitted with the constant  $\beta$ ,  $n$ .

A fitted curve using C1 and C2 was illustrated in Figure 9 and the fitting results were clarified in Table 5. The mean values of  $A'$ ,  $\beta$ ,  $n$  within 95% confidence bounds were  $4.744 \times 10^{-10}$ , 1.539, and 0.676 respectively, and the R-squared value was 0.9965. The model was validated with high accuracy in terms of R-squared value. Fitted curves for C3 and M1 were illustrated in Figure 10 and the fitting results were clarified in Table 6. Using the same  $\beta$  and  $n$  (1.539, 0.676),  $A'$  were fitted to  $3.839 \times 10^{-11}$  and  $7.511 \times 10^{-10}$  respectively. The models were also validated with high accuracy in terms of R-squared value; 0.9933 and 0.9826. From the result, the hypothesis was verified that the degradation behaviors of IGBTs with same technology are consistent among the different companies. In summary, the degradation of a trench gate field stop IGBT subjected to ESD damage can be predicted using the proposed degradation models with the degradation rate ( $A'$ ) fitted for the experimental results of the samples.

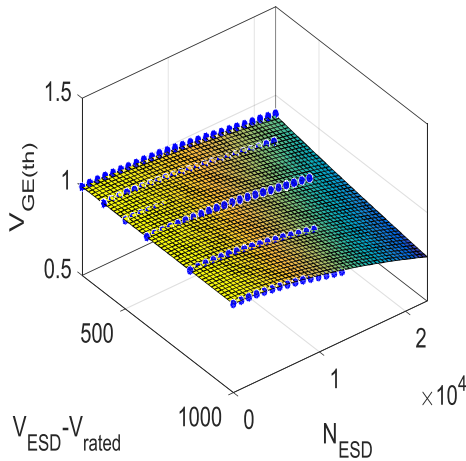


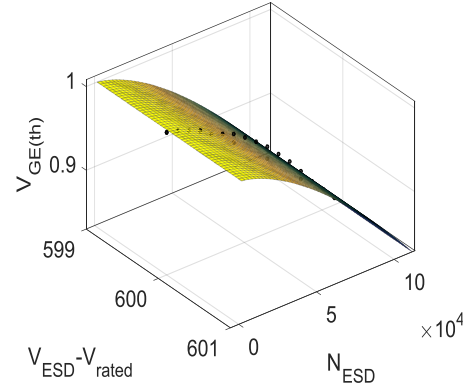
Figure 9. Orthogonal view of the  $V_{th}$  degradation model fitted with C1 and C2 data

Table 5. The coefficients and R-squared value of  $V_{th}$  degradation model fitted with C1 and C2

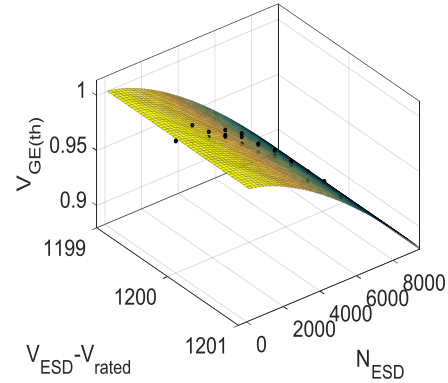
Coefficients (with 95% confidence bounds)		R-squared value
$A'$	$4.744 \times 10^{-10}$ ( $3.682 \times 10^{-10}$ , $5.805 \times 10^{-10}$ )	
$\beta$	1.539 (1.522, 1.557)	
$n$	0.676 (0.661, 0.690)	

Table 6. The coefficients and R-squared values of  $V_{th}$  degradation models fitted with C3 and M1 respectively

	$A'$	$\beta$	$n$	$R^2$
C3	$3.839 \times 10^{-11}$	1.539	0.676	0.9933
M1	$7.511 \times 10^{-10}$			0.9826



(a)



(b)

Figure 10. Orthogonal view of  $V_{th}$  degradation model: (a) C3 and (b) M1

## 5. CONCLUSION

This paper determined the key failure precursor for IGBTs subjected to electrical stresses. Then, the empirical model was proposed to describe the evolution of the failure precursor during the degradation. The main contribution of this study is that the degradation of IGBTs that is modeled by emulating the degradation of IGBTs. The degraded IGBTs were prepared by injecting artificial faults of electrostatic discharge (ESDs). The previous studies only compared the conditions of normal IGBTs with the conditions of failed ones.

The failure precursor  $V_{GE(th)}$  for degradation of IGBTs subjected to C-G ESD damage was identified and the corresponding degradation model was constructed. The performance of  $V_{GE(th)}$  was verified using three sets of IGBTs components and one set of IGBT modules. We concluded that the proposed model properly describes the degradation of IGBTs subjected to electrical stresses. In the future study, another relevant precursor will be identified, and the performance of the precursor will be validated in the case that the IGBTs experience degradation by E-G ESD damage.

**ACKNOWLEDGEMENT**

This work was supported by grants from Hyundai NGV (Next Generation Vehicle) through a program named as “Development of prognostic technique for electronic components in inverter system” by Hyundai Motor Group.

**REFERENCES**

- Baliga, B. J., Adler, M. S., Love, R.P., Gray, P. V., & Zommer, N. D. (1984). The insulated gate transistor: A new three-terminal MOS-controlled bipolar power device. *IEEE Transactions on Electron Devices*, 31 (6), 821-828. Doi:10.1109/T-ED.1984.21614
- Celnikier Y., Benabou, L., Dupont, L., & Coquery, G. (2011). Investigation of the heel crack mechanism in Al connections for power electronics modules. *Microelectronics Reliability*, 51 (5), 965-974. doi:10.1016/j.microrel.2011.01.001
- Jeong, J.-S., Hong, S.-H., & Park, S.-D. (2007). Field failure mechanism and improvement of EOS failure of integrated IGBT inverter modules. *Microelectronics Reliability*, 47 (9-11), 1795-1799. doi:10.1016/j.microrel.2007.07.087
- Lee, J., Oh, H., Park, C. H., Youn, B. D., Kim, D. H., Kim, B. H., & Cho, Y. U. (2016). Fault injection to insulated gate bipolar transistor (IGBT) using electrostatic discharge. *Proceeding of Korean Society of Mechanical Engineers* (8), April 27-29, Busan, Korea.
- Oh, H., Han, B., McCluskey, P., Han, C., & Youn, B. D. (2015). Physics-of-failure, condition monitoring, and prognostics of insulated gate bipolar transistor modules: A review. *IEEE Transactions on Power Electronics*, 30 (5), 2413-2426. doi:10.1109/TPEL.2014.2346485
- Patil, N., Celaya, J., Das, D., Goebel, K., & Pecht, M. (2009). Precursor parameter identification for insulated gate bipolar transistor (IGBT) prognostics. *IEEE Transactions on Reliability*, 58 (2), 271-276. doi:10.1109/TR.2009.2020134
- Shringarpure, R., Venugopal, S., Li, Z., Clark, L. T., Allee, D. R., Bawolek, E., & Toy, D. (2007). Circuit simulation of threshold-voltage degradation in a-Si: H TFTs fabricated at 175 °C. *IEEE Transactions on Electron Devices*, 54 (7), 1781-1783. doi:10.1109/TED.2007.899667
- Wysocki, P., Vashchenko, V., Celaya, J., Saha, S., & Goebel, K. (2009). Effect of electrostatic discharge on electrical characteristics of discrete electronic components. *Annual Conference of the Prognostics and Health Management Society* (1-10), September 27-October 1, San Diego.
- Yang, S., Bryant, A., Mawby, P., Xiang, D., Ran, L., & Tavner, P. (2011). An industry-based survey of reliability in power electronic converters. *IEEE Transactions on Industry Applications*, 47 (3), 1441-1451. Doi:10.1109/TIA.2011.2124436
- Zhou, L., Zhou, S., and Xu, M. (2013). Investigation of gate voltage oscillations in an IGBT module after partial bond wires lift-off. *Microelectronics Reliability*, 53 (2), 282-287. doi:10.1016/j.microrel.2012.08.024
- Zhou, S., Zhou, L., and Sun, P. (2013). Monitoring potential defects in an IGBT module based on dynamic changes of the gate current. *IEEE Transactions Power Electronics*, 28 (3), 1479-1487. doi:10.1109/TPEL.2012.2210249